Astron. Astrophys. 339, 327–336 (1998)

ASTRONOMY AND ASTROPHYSICS

1H0419-577: a "two-state" soft X-ray Seyfert galaxy⋆

M. Guainazzi[1,2], A. Comastri[3], G.M. Stirpe[3], W.N. Brandt[4], F. Fiore[5,2], K.M. Leighly[6], G. Matt[7], S. Molendi[8], E.M. Puchnarewicz[9], L. Piro[10], and A. Siemiginowska[11]

[1] Astrophysics Division, Space Science Department of ESA, ESTEC, Postbus 299, 2200 AG Noordwijk, The Netherlands
[2] *Beppo-SAX* Science Data Center, c/o Nuova Telespazio, Via Corcolle 19, I-00131 Roma, Italy
[3] Osservatorio Astronomico di Bologna, Via Zamboni 33, I-40126 Bologna, Italy
[4] Department of Astronomy and Astrophysics, Penn State University, 525 Davey Lab, University Park, PA 16802, USA
[5] Osservatorio Astronomico di Roma, Via dell'Osservatorio 5, I-00040 Monteporzio-Catone (RM), Italy
[6] Columbia Astrophysical Laboratory, Columbia University, 538 West 120th Street, New York, NY 10027, USA
[7] Dipartimento di Fisica, Università degli Studi "Roma 3", Via della Vasca Navale 84, I-00146 Roma, Italy
[8] Istituto di Fisica Cosmica e Tecnologie Relative/C.N.R., Via Bassini 15, I-20133 Milano, Italy
[9] Mullard Space Science Laboratory, University College London, Holmbury St.Mary, Dorking, Surrey RH5 6NT, UK
[10] Istituto di Astrofisica Spaziale - C.N.R., Via Fosso del Cavaliere, I-00133 Roma, Italy
[11] Harvard-Smithsonian Center for Astrophysics,60 Garden St., Cambridge, MA 02138, USA

Received 4 March 1998 / Accepted 15 July 1998

Abstract. In this paper we report on the first simultaneous optical and X-ray (Beppo-SAX) observations of the radio-quiet AGN 1H0419-577. The optical spectrum clearly leads us to classify this source as a Seyfert 1. The X-ray spectrum is, however, somewhat at odds with this classification: a simple flat ($\Gamma \sim 1.55$) and featureless power-law is a good description of the whole 1.8-40 keV spectrum, even if the upper limit to a broad iron line is not very tight. An analysis of a still unpublished ROSAT observation of the same target reveals that the soft X-ray spectrum has undergone a transition from a steep ($\Gamma = 2.5$) to a flat ($\Gamma = 1.55$) state, at least in the 0.7-2 keV band. If this difference is due to a remarkably variable soft excess, it is unlikely that a single component is responsible for the optical/UV/soft X-ray spectral distribution. The hypothesis that the difference is due to a change in the primary X-ray continuum and its implications for current Comptonization models are discussed.

Key words: X-rays: galaxies – galaxies: Seyfert – galaxies: individual: 1H0419-577

1. Introduction

Soon after it was discovered that the X-ray spectra of Seyfert 1 galaxies can be described at 0-th order by a simple power-law (Mushotzky 1984), it became clear that significant deviations exist from this simple behavior. In particular, a *soft excess* above the extrapolation of the high-energy power-law was observed by all the main X-ray missions in the 80s: HEAO-1 (Pravdo et al. 1981; Singh et al. 1985), EXOSAT (Arnaud et al. 1985; Turner & Pounds 1989), Einstein (Kruper et al. 1990; Turner et al. 1990), BBXRT (Turner et al. 1993). Optical/UV and soft X-ray emissions are generally well correlated (Walter & Fink 1993; Puchnarewicz et al. 1996; Laor et al. 1997) and this has traditionally supported the idea that they are one and the same spectral component, probably originating as thermal emission in an accretion disk (Czerny & Elvis 1987). However, thin disc models generally fail to reproduce the observed Spectral Energy Distribution (SED, Ulrich & Molendi 1996; Laor et al. 1997). Moreover, the tight correlation between optical and UV variations in some Seyfert galaxies (Peterson et al. 1991, Clavel et al. 1991) argues against an origin as a thermal emission from accretion discs. If irradiation of the disc by a high-energy external source is taken self-consistently into account, the agreement between data and models improves (Molendi et al. 1992, Siemiginowska et al. 1995). There is nowadays formidable evidence that reprocessing of the primary radiation indeed occurs on μpc scale around the nuclei of Seyfert 1s, either from neutral (Pounds et al. 1990, Piro et al. 1990, Nandra & Pounds 1994, Nandra et al. 1997a) or ionized (Piro et al. 1997) matter.

Given this framework, we discuss in this paper the results of a Beppo-SAX observation of the radio-quiet AGN 1H0419-577 (1ES 0425-573), along with the analysis of a still unpublished pointed PSPC observation, which was performed four years earlier. 1H0419-577 is classified as a Seyfert 1 by Brissenden (1989) and as a Seyfert 1.5 by Grupe (1996). A high-quality optical spectrum was taken the same night as the Beppo-SAX observation, and the relevant results are presented in this paper.

1H0419-577 is a moderately distant ($z = 0.103$) object. It is one of the brightest extragalactic sources in the EUVE catalog, with flux $F = 3.6 \times 10^{-12}$ erg cm^{-2} s^{-1} in the 58-174 Åband (Marshall et al. 1995, Fruscione 1996). It is also included in the Seyfert soft X-ray selected sample of Grupe et al. (1998,

Send offprint requests to: M. Guainazzi, (mguainaz@astro.estec.esa.nl)

⋆ Partly based on observations collected at the European Southern Observatory, La Silla, Chile

RXJ0426-57). No significant radio emission is reported, the upper limit on the 8.4 GHz flux being 3.6 mJy (Brissenden 1989). Despite the fact that it is a relatively bright source in X-ray (it was detected by HEAO A-2, Mushotzky 1995, private communication), its X-ray properties have not been well studied yet.

The paper is organized as follows: in Sect. 2 the optical data are presented. Reduction and analysis of the Beppo-SAX data are presented in Sect. 3 and Sect. 4 respectively. In Sect. 5 the PSPC data are analyzed and the relevant outcomes are compared with Beppo-SAX ones. The discussion of the main results is given in Sect. 6. Sect. 7 summarizes the main conclusions. $H_0 = 75$ km s^{-1} Mpc^{-1} is assumed throughout the paper. Preliminary results have been published in Guainazzi et al. (1998).

2. The optical spectrum

Optical spectra of 1H0419−577 were obtained at the ESO 1.52m telescope on 1996 October 1 and 2, using the Boller & Chivens spectrograph with a 127mm camera and a Loral/Lesser thinned CCD with 2048×2048 pixels. The pixel size is 15μm, and the projected scale on the detector 0.82 arcsec pixel^{-1}. The grating used has 600 grooves mm^{-1}. The spectra were obtained through a 2-arcsec wide slit, at a resolution of 4.6 Å. Both nights were photometric. Two integrations of 1800 seconds each were obtained.

Standard techniques were used to reduce the spectra, using the NOAO IRAF package. In particular, the spectrophotometric calibration of the spectra was perfected through their comparison with, and broad-band normalized to, short exposures of 1H0419−577 obtained during the same nights through an 8 arcsec slit. This allowed us to correct the narrow-slit spectra for light losses and differential refraction. The two spectra were averaged and yielded the final spectrum shown in Fig. 1. Because the calibration curves of the two nights and the individual spectra coincide within < 5%, we consider the spectrophotometric quality of the final spectrum to be of this order.

The spectrum displays characteristics typical of Seyfert 1 galaxies, with strong broad permitted lines and narrow forbidden lines. Table 1 lists the fluxes, equivalent widths, and FWHM of the main lines. In order to obtain these measurements a 1st order pseudo-continuum was fitted to the local minima bracketing each line. In most permitted lines the broad component was isolated by modeling the narrow line contribution with a suitably scaled profile of the [O III]λ5007 line. Each scaling factor was determined on the basis of the smoothest residual broad profile. The corresponding line fluxes in Table 1 are thus simply the [O III]λ5007 flux multiplied by the respective scaling factors. In addition, the contaminating lines were subtracted from Hα and Hβ using a scaled [O III]λ5007 profile for the narrow lines ([O III]λ4959, [N II]λ6548 and λ6584) and a scaled broad-Hα profile for the broad lines (He II λ4686 and Fe II λ4924). The Fe II lines are weaker than average for a Seyfert 1: the ratio between the integrated fluxes of the 4570 Å (rest wavelength) blend and of Hβ is lower than 0.1 (cfr. Joly 1988).

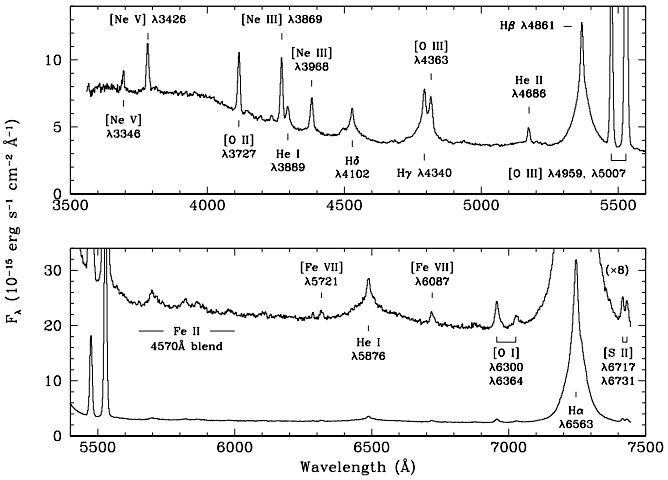

Fig. 1. The optical spectrum of 1H0419−577 obtained in 1996 October. The spectrum has been displayed in two parts for clarity, and the red part (bottom panel) is also shown magnified by a factor 8 to enhance the weaker lines. The main optical lines are indicated on the plot. The wavelength scale is in the rest system of the observer (z=0.103).

Table 1. Integrated fluxes, FWHM, and equivalent widths of the main optical emission lines

Line	Flux (erg/s/cm^2)	FWHM (km/s)	EW (Å)
[Ne V]λ3346	1.1×10^{-14}	620	2
[Ne V]λ3426	3.6×10^{-14}	760	5
[O II]λ3727	4.8×10^{-14}	750	8
[Ne III]λ3869	5.7×10^{-14}	770	11
He I λ3889 + Hζ	2.4×10^{-14}	1090	5
[Ne III]λ3968 + Hη	4.7×10^{-14}	950	10
Hδ + [S II]λ4068,λ4076	7.7×10^{-14}	1500	18
Hγ broad	1.9×10^{-13}	3470	51
Hγ narrow	2.0×10^{-14}	560	5
[O III]λ4363	2.3×10^{-14}	670	6
He II λ4686 broad	2.4×10^{-14}	3720	7
He II λ4686 narrow	1.2×10^{-14}	600	4
Hβ broad	4.7×10^{-13}	3460	146
Hβ narrow	5.0×10^{-14}	560	16
[O III]λ4959	1.7×10^{-13}	560	53
[O III]λ5007	5.0×10^{-13}	560	160
He I λ5876 broad	8.4×10^{-14}	4650	32
He I λ5876 narrow	5.0×10^{-15}	560	2
[Fe VII]λ6087	4.0×10^{-15}	730	2
[O I]λ6300	9.7×10^{-15}	720	4
[O I]λ6364	3.4×10^{-15}	720	1
Hα broad	1.6×10^{-12}	2660	704
Hα narrow	1.1×10^{-13}	560	50
[S II]λ6717	6.6×10^{-15}	460	3
[S II]λ6731	6.7×10^{-15}	460	3

The spectrum is in broad agreement with the one presented by Brissenden (1989) and confirms unambiguously the classification of 1H0419-577 as a Seyfert 1.

3. Beppo-SAX data reduction

Beppo-SAX (Boella et al. 1997a) is a major mission of the Agenzia Spaziale Italiana (ASI), with participation of the Netherlands Agency for Aerospace Programs (NIVR); it aims to study celestial sources in the wide X-ray band 0.1-300 keV. The scientific payload is constituted of a pair of gas scintillator proportional counters with imaging capabilities (Low Energy Concentrator Spectrometer, LECS, Parmar et al. 1997, sensitive in the 0.1-10 keV band; Medium Energy Concentrator Spectrometer, MECS, Boella et al. 1997b, sensitive in the 1.8-10.5 keV band), and a pair of collimated high-energy instruments (High Pressure Gas Scintillating Proportional Counter, HPGSPC, Manzo et al. 1997, sensitive in the 7-60 keV band; Phoswitch Detector System, PDS, Frontera et al. 1997, sensitive in the 13-200 keV band). The HPGSPC is more oriented to high-resolution spectroscopy of bright sources, while the PDS possesses an unprecedented sensitivity in its energy range (Guainazzi & Matteuzzi 1997).

Beppo-SAX observed 1H0419-577 on 1996 September 30, from 06:24:00 UT to 16:40:50 UT. The LECS was switched off during the whole observation due to technical problems. The other instruments were operating in direct modes, which provide full information on the arrival time, energy, burst length/rise time and - if available - position of each photon. Data have been reduced with the SAXDAS package (version 1.1) in the FTOOLS 3.5 environment. Standard selection criteria on satellite aspect quantities were applied to avoid Earth occultation (angle between the pointing direction and the Earth's limb $\geq 5^\circ$); South Atlantic Geomagnetic Anomaly (SAGA) passages; and particle contamination (momentum associated to the Geomagnetic cut-off Rigidity ≥ 6 GeV/c). In the MECS image, the source is nearly on-axis (offset angle $\lesssim 1'$). MECS scientific products have been extracted from a circular area 3' radius around the apparent centroid of the source. Background spectra have been extracted from blank sky fields, using the same extraction region in detector coordinates as the source. Appropriate response matrices have been created, using the calibration files publicly available since 1997 January 31, which include the results of on-flight calibration. Total net MECS exposure time is $T \simeq 22600$ s and the corresponding count rate is 0.171 ± 0.003 s^{-1} in the whole energy band. The spectrum has been rebinned in order to have at least 20 counts per channel, to ensure the applicability of χ^2 statistics. The source is not detected in the HPGSPC. PDS data have been further screened by eliminating 5 minute intervals after any SAGA passage, in order to avoid gain instabilities due to recovery to the nominal values after instrument switch off. The PDS was working in rocking mode, each collimator pointing alternatively every 96 seconds to the source and a field $\pm 3.5^\circ$ aside. Short-lived ($\tau \lesssim 1$ s) spikes, due to particle "bursts" along the orbit, were also removed, according to the following procedure: bins in the 2-seconds binned light curves of each detector, whose count rate exceeded the mean by 5 standard deviations, have been excluded from the scientific product accumulation. Net exposure time in the PDS results $\sim$ one half of the MECS ($\simeq 10700$ s). In the 13-36 keV band the net background-subtracted count rate is 0.129 ± 0.052 s^{-1}; a typical systematic uncertainty of ~ 0.02 s^{-1} in the whole 13-200 keV PDS band has been taken into account hereinafter. (Guainazzi & Matteuzzi 1997). The 13-36 keV detection is significant at the 5 σ level.

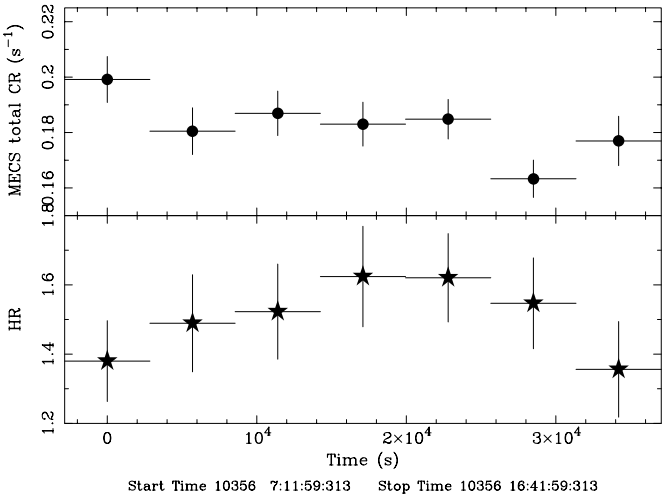

Fig. 2. Broadband (*i.e.* 1.8-10.0 keV) MECS light curve (*upper panel*) and ratio (*lower panel*) between the 3-10.5 and 1.8-3.0 keV bands count rates. Binning time is $\Delta t = 5700$ s, corresponding approximately to one Beppo-SAX orbit.

Data analysis has been performed using the XANADU package. Hereafter energies are quoted in the source rest frame and errors are 90% confidence level for one interesting parameter (*i.e.* $\Delta\chi^2 = 2.71$), unless otherwise specified.

4. Beppo-SAX data analysis

4.1. Timing analysis

In Fig. 2 the full energy band MECS light curve of the Beppo-SAX observation is shown. It displays a smooth decreasing trend of $\simeq 15\%$ during the $\sim 3.5\times10^4$ s of elapsed time. The hardness ratio between the count rates in the 1.8-3.0 and 3.0-10.5 keV bands (see Sect. 4) shows a regular trend, increasing in the first 2×10^4 s and decreasing thereafter. However, the χ^2 for constant hypothesis is 4 over 6 degrees of freedom only. We extracted spectra during the time intervals when the HR is higher or lower than the mean value. The difference in the spectral indices of a simple power-law model between the two states is $\simeq 0.06$, comparable with the statistical uncertainties. We will therefore focus in the following on the time-averaged spectral behavior to achieve the maximum S/N ratio.

4.2. Spectral analysis

A simple power-law with photoelectric absorption by cold matter is a rather good representation of the MECS spectrum (see Fig. 3). If the absorbing column density is left free to vary, $N_H < 2.3\times10^{21}$ cm^{-2}. N_H has been therefore constrained to be not lower than the Galactic value along the 1H0419-577

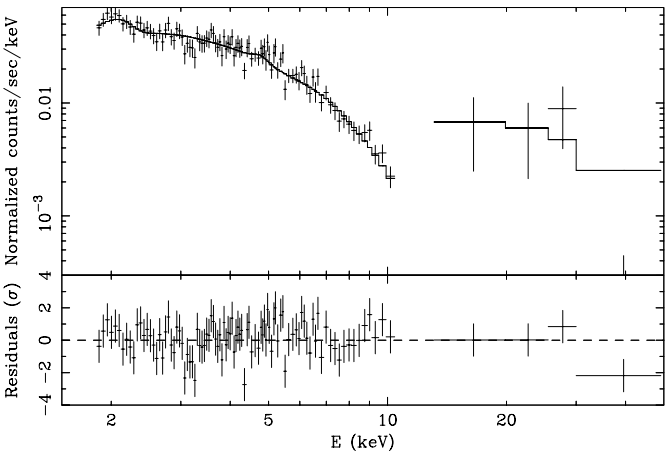

Fig. 3. Spectrum (*upper panel*) and residuals in units of standard deviations (*lower panel*) when a simple power-law model with photoelectric absorption by cold matter is applied to the MECS and PDS data simultaneously. Each of the PDS data points has a S/N > 1.5, each of the MECS data points a S/N > 5.

line of sight ($N_{H_{Gal}} = 2 \times 10^{20}$ cm^{-2}, Dickey & Lockman 1990) and is always consistent with its minimum allowed value. The χ^2 is formally acceptable ($\chi^2 = 114/124$ d.o.f.). The spectral index is rather flat ($\Gamma_{3-10keV} = 1.51^{+0.09}_{-0.12}$) if compared with the mean value for the Seyfert 1 Galaxies ($\Gamma_{3-10keV} = 1.91 \pm 0.07$, Nandra et al. 1997a) observed by ASCA. The unabsorbed flux in the 2-10 keV band is $F = (1.1 \pm 0.2) \times 10^{-11}$ erg s^{-1} cm^{-2} (~ 0.5 mCrab), corresponding to a luminosity $L \simeq 5.3 \times 10^{44}$ erg s^{-1}, which ranks 1H0419-577 among the most luminous Seyfert 1s in X-rays. The normalization at 1 keV is $(2.32 \pm 0.12) \times 10^{-3}$ photons cm^{-2} s^{-1}.

If we superimpose the PDS points to the power-law best fit, they lie well on the power-law extrapolation ($\chi^2 = 131/153$ d.o.f.), provided the usual relative normalization constant $C_{PDS/MECS} = 0.80$ between MECS and PDS flux at 1 keV is assumed (Cusumano et al. 1998). The results are not affected by the residual $\pm 10\%$ uncertainty on $C_{PDS/MECS}$.

Although we have not found clear evidence of any deviation from the simple power-law behavior, we have searched for narrow line emission features and/or changes in the continuum curvature in the broadband spectrum. If a broken power-law is used instead of a simple power-law, the χ^2 is only marginally better [F-test (F) equal to 2.6, significant at only 96.0%]. We have also tried a more physical double power-law model, which results in a (basically unconstrained) very steep soft component and a $\Delta\chi^2 = 4.1$. Although the improvement in the quality of the fit is not statistically negligible (99.7% significance level), an inspection by eye of the residuals (see Fig. 3) reveals that such a solution tends to account for the behavior of the lowest energy channels in the MECS bandpass. The deviation expressed in data/model ratio is there $\sim 10\%$, *i.e.* of the same order of the calibration uncertainties; moreover, the feature below 2 keV is *not* the widest regular one in the residuals spectrum. We consider therefore such evidence as scarcely conclusive and will search for more robust and calibration-independent tests for it.

The attempts at modeling the slight concavity of the spectrum at low energy either with thermal or partial covering models were even less successful. Table 2 reports a summary of the fit results.

Broad K_α fluorescent lines from neutral or low-ionized iron have been detected in almost all the Seyfert 1s observed by Ginga (Nandra & Pounds 1994) and ASCA (Nandra et al. 1997a) so far. Adding a narrow (*i.e.* $\sigma = 0$) Gaussian emission profile to the simple power-law model improves only marginally the fit ($F = 1.9$, significant at 84.6%). If the centroid energy of the line is frozen at 6.4 keV (neutral iron) or 6.7 keV (He-like iron), the equivalent widths (EW) are $EW_{6.4\ keV} = 17^{+83}_{-17}$ eV and $EW_{6.7\ keV} = 70^{+90}_{-70}$ eV respectively. If the widths of the lines are allowed to vary as free parameters, the decrease of the χ^2 in comparison to the narrow-line case is always negligible ($\Delta\chi^2 < 1$). When the widths of the lines are held fixed to the mean in Nandra et al. sample (430 eV, 1997a), the upper limits on the EW are $\simeq 250$ eV.

Flattened spectra can be produced if a Compton reflection component is superimposed on a steeper intrinsic continuum. This hypothesis is supported in Seyfert galaxies by the flattening of the continuum shape at $E \gtrsim 10\ keV$ observed by Ginga (Pounds et al. 1990, Piro et al. 1990) and by the detection of broad fluorescent iron lines (Tanaka et al. 1995; Nandra et al. 1997a), which are considered to be signatures of reprocessing of the nuclear X-rays by optically thick matter, possibly in the form of a rotating accretion disk around the central black hole. We have tested such an hypothesis with the model `pexrav` in XSPEC, leaving as free parameters only the intrinsic spectral index and the relative normalization R between the direct and the reflected component. The other parameters are basically unconstrained and we have therefore fixed the cut-off energy of the direct spectrum at $E_{cut-off} = 100$ keV (Gondek et al. 1996) and the angle between the disk axis and the line-of-sight at 30° (Nandra et al. 1997a). The improvement of the fit is significant at 98.4% ($F = 5.9$), and the intrinsic photon index turns out to be even steeper than typical values observed in Seyfert galaxies ($\Gamma \simeq 2.15$). The nominal best-fit values correspond to an unplausibly high amount of reflection ($R = 10$) but the spectral parameters are basically unconstrained. The upper limits on the EW of a narrow iron line added to such a continuum are $EW_{6.4\ keV} < 40$ eV and $EW_{6.7\ keV} < 90$ eV in the "neutral" and "ionized" cases, respectively. Leaving the widths of the lines free results in no (*i.e.* $\Delta\chi^2 = 0$) further improvement. If we fix the intrinsic spectral index to the average value found by Nandra et al. (1997a), $R = 3.8 \pm 0.9$, whereas the EW of a narrow (broad) neutral fluorescent line is < 110 (200) eV. It is therefore unlikely that the line originates in the same relativistic X-ray illuminated disc which could be advocated as the responsible for the huge continuum reflection component, unless the disc is substantially ionized. We consider hereafter a simple power-law with photon index $\Gamma \simeq 1.55$ the best modeling of the spectral shape in the whole 1.8-40 keV band.

Table 2. Results of the simultaneous fits of MECS and PDS data. A photoelectric absorption from cold matter with $N_H = N_{H_{Gal}} = 2 \times 10^{20}$ cm^{-2} was added to all the quoted models. PO=power-law, BKNPO=broken power-law, GA=Gaussian line.

Panel a: power-laws continuum modeling					
Model	Γ	Γ_{soft}	E_{break} (keV)	N_{soft}/N_{hard}	χ^2/d.o.f.
PO	1.61 ± 0.06	...	...	...	130.6/153
BKNPO	1.56 ± 0.10	1.8 ± 0.4	3.0 ± 1.0	...	128.0/151
PO+PO	1.55 ± 0.09	$7^{\ddagger}$	...	$3.7^{\ddagger}$	126.5/150
Panel b: iron line emission					
Model	Γ	E (keV)	σ (keV)	EW (eV)	χ^2/d.o.f.
PO+GA	$1.64^{+0.09}_{-0.08}$	$6.2^{\ddagger}$	$0.7^{\ddagger}$	$180^{\ddagger}$	128.1/151
Narrow neutral line	$1.61^{+0.07}_{-0.06}$	$6.4^{\dagger}$	$0^{\dagger}$	17^{+83}_{-17}	130.6/152
Broad neutral line	1.65 ± 0.08	$6.4^{\dagger}$	$0.43^{\dagger}$	< 250	128.4/151
Narrow ionized line	$1.63^{+0.06}_{-0.07}$	$6.7^{\dagger}$	$0^{\dagger}$	70^{+90}_{-70}	129.1/152
Broad ionized line	$1.63^{+0.10}_{-0.07}$	$6.7^{\dagger}$	$0.43^{\dagger}$	< 260	129.1/151

‡unconstrained
‡fixed

5. ROSAT PSPC observation

5.1. ROSAT data analysis

In order to cope with the lack of information at energies lower than $\simeq 2\ keV$, we have analyzed a still unpublished ROSAT PSPC observation of the same target. 1H0419-577 was observed by ROSAT on 1992 April 7, for a total exposure time of 4094 seconds. Source spectra have been extracted from a circular region of 2'45" radius around the centroid of the source, while background spectra have been extracted from an annulus of internal and external radii 6'20" and 8'30" respectively. The radii have been chosen in order to avoid six serendipitous sources that have been detected in the field of view. To perform spectral fitting, an appropriate PSPC-B redistribution matrix for the observation date (`pspcb_gain2.rmf`) has been used and the effective area calculated with the software tool `pcarf` included in FTOOLS 3.6. Spectral PI channels lower than 11 ($E \lesssim 0.15$ keV) and higher than 32 ($E \gtrsim 2.1$ keV) in the rebinned spectrum have been excluded from the spectral analysis. The resulting net count rate is 5.72 ± 0.04 s^{-1}; background contributes less than 1/30 for each spectral channel.

The broadband 0.1-2.4 keV light curve shows a slight (*i.e.* $\sim 5\%$) tendency to increase with time. We have investigated whether such a trend could be associated to spectral variability by studying the light curves in the 0.1-0.5 keV and 0.5-2.0 keV energy bands (see Fig. 4). The suggestion of a wider dynamical range of the soft light curve variation is only marginal. In the following we will therefore focus on the average spectral behavior only.

A simple power-law with photoelectric absorption yields a formally acceptable fit ($\chi^2_r = 0.92$). $\Gamma = 2.67 \pm 0.05$ and the 1 keV normalization is $1.03 \pm 0.03 \times 10^{-2}$ photons cm^{-2} s^{-1}. The residuals show however a regular wavy trend (see Fig. 5). This trend cannot be removed with a linear adjustment of the instrumental gain, as achievable with the command `gain` in XSPEC. We checked therefore the statistical significance of

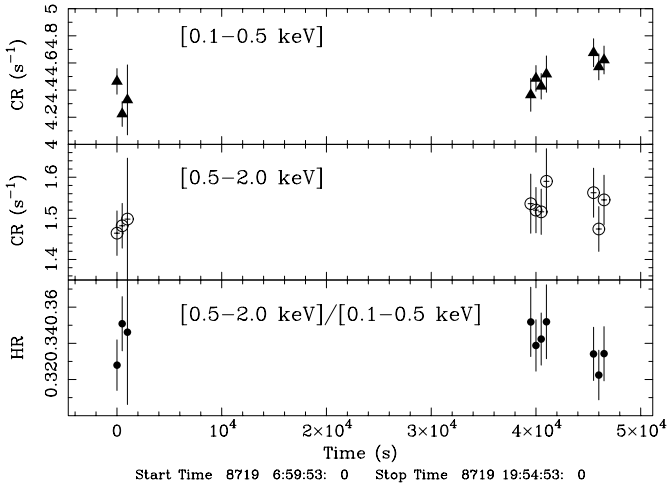

Fig. 4. PSPC 1H0419-577 light curves in the 0.1-0.5 keV (*upper panel*) and 0.5-2.0 keV (*central panel*) bands, and their hardness ratio (*lower panel*). Binning time is $\Delta t = 500$ s. The panels are displayed in the same relative ordinate scale to allow direct comparison of the dynamical ranges.

spectral complexity. An absorption edge (with energy broadly consistent with the photoionization threshold energy for O VII), a thermal optically thin or thick emission or a break in the power-law shape yield a comparable improvement of the χ^2 ($\Delta\chi^2 = 9.7 - 12.3$ for two further degrees of freedom, corresponding to a confidence level $\gtrsim$ 99.97-99.99%). There is therefore a suggestion of soft X-ray spectral complexity, with an ultrasoft component emerging below $\simeq 0.5\ keV$, or, alternatively, an absorption edge due to highly ionized interposed matter. In some fits, the best-fit N_H value is significantly lower than the Galactic N_H in the direction of 1H0419-577 (2.0×10^{20} cm^{-2}), however not inconsistent with it if we take into account a conservative estimate of the uncertainties on the nominal Galactic values of 20-30% (*i.e.*: 5×10^{19} cm^{-2}, Dickey & Lockman 1990). An investigation of the spectral complexity in the soft X-ray spectrum

Table 3. Best-fit results of the ROSAT PSPC spectral analysis. PO=power-law, ED=absorption edge, BKNPO=broken power-law, BB=blackbody, BREMS=thermal bremsstrahlung.

N_H free Model	N_H (10^{20} cm^{-2})	Γ_{soft}	$\Gamma_{ultrasoft}$ or τ	E or kT (eV)	χ^2/d.o.f.
PO	1.42 ± 0.11	$2.71\pm^{+0.05}_{-0.06}$	...	...	20.1/17
PO+BB	$1.3^{+0.3}_{-0.2}$	$2.51^{+0.14}_{-0.16}$	...	73^{+12}_{-29}	9.8/15
PO+BREMS	$1.5^{+0.3}_{-0.2}$	$2.51^{+0.15}_{-0.27}$	...	150^{+60}_{-90}	10.4/15
BKNPO	$1.64^{+0.19}_{-0.17}$	$2.54^{+0.12}_{-0.18}$	$2.88^{+0.22}_{-0.12}$	700^{+300}_{-200}	9.9/15
PO+PO	$1.8^{+1.2}_{-0.4}$	$2.4^{+4.8}_{-2.4}$	$3.9^{+3.4}_{-3.9}$	...	11.1/15
ED*PO	$1.53^{+0.15}_{-0.13}$	2.71 ± 0.07	0.29 ± 0.15	0.67 ± 0.10	8.8/15

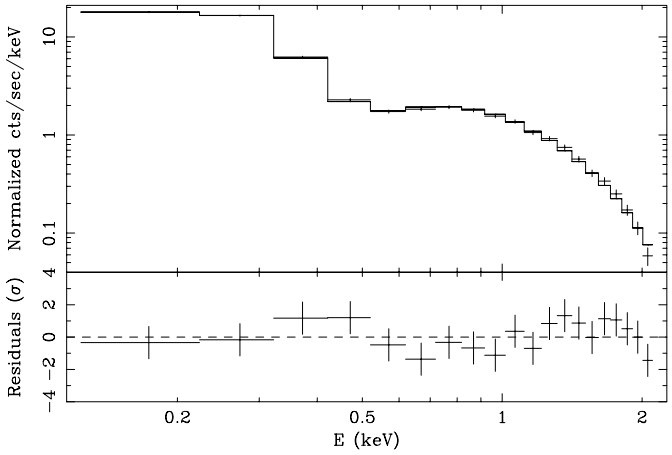

Fig. 5. Spectrum (*upper panel*) and residuals (*lower panel*) in units of standard deviations when a simple absorbed power-law model is applied to the ROSAT PSPC data of 1H0419-577.

would require much better spectroscopic quality and/or simultaneous monitoring of the soft and hard X-ray. However, we stress that the ROSAT/PSPC spectrum *is always much steeper than the MECS one*, regardless of the specific model adopted. $\Delta\Gamma \equiv \Gamma_{PSPC} - \Gamma_{MECS} = \Gamma_{soft} - \Gamma_{hard}$ (see Sect. 4) ranges from 0.8 to 1.3.

We investigated also whether we could get comparably good fits if an underlying MECS-like power-law is assumed. We than fitted the PSPC spectrum with two-components models, where one of the components is a power-law with photon index held fixed at 1.55 and free normalization. The only case for which an acceptable χ^2 is obtained is the double power-law model, which yields: $\chi^2 = 11.8/16$ d.o.f., $\Gamma_{soft} = 3.01 \pm 0.18$ and $N_H = (1.7 \pm 0.2) \times 10^{20}$ cm^{-2}. It is better than the single power-law model at the 99.6% level of confidence (cfr. first row in Table 3). The ratio between the "hard" power-law normalization as measured by the MECS and PSPC is 1.1 ± 0.5. On the other hand, adding a MECS-like power-law to the other models listed in Table 3 yields a negligible (*i.e.*: $\Delta\chi^2 < 1$) improvement of the quality of the fit. In particular, a double blackbody + power-law model with photon index held fixed to the high-energy measured value - which have often been used to approximate the superposition of a high-energy non-thermal continuum and a disc emission - is not a viable model ($\chi^2 = 76.8/14$ d.o.f.).

5.2. ROSAT PSPC/Beppo-SAX MECS comparison

Beppo-SAX observed 1H0419-577 about four years later than ROSAT. The source was caught with very different spectral properties; namely the ROSAT PSPC 1992 spectrum is much steeper than the 1996 Beppo-SAX MECS one.

Recently, several authors have pointed out that the spectral indices as measured by the PSPC are systematically steeper than measured by other missions with a sensitivity bandpass extending at higher energies. The amount of such a difference has been estimated between 0.2 (Turner 1993, Fiore et al. 1994) and 0.4 (Iwasawa et al. 1998). It cannot therefore account completely for the observed difference. Moreover, If we fit the PSPC data with a power-law of index $\Gamma = 2.0$ and a blackbody component, the χ^2 turns out to be unacceptably high (439/16 d.o.f.). However, a double power-law model with one of the photon index held fixed to 2.0 yields $\chi^2 = 11.4/16$ d.o.f., with $N_H = (1.7 \pm 0.2) \times 10^{20}$ cm^{-2} and $\Gamma_{soft} = 3.2 \pm 0.3$.

The energy interval where the two PSPC and the MECS are well calibrated and overlap (1.8-2.0 keV) is too narrow to allow a direct comparison of the spectra via standard fitting techniques.

In order to partly overcome such problems, we studied the ratio between the PSPC and MECS 1H0419-577 spectra and the corresponding spectra of the featureless radio-loud quasar 3C273, whose X-ray spectrum is known to be well represented by a simple power-law in the whole 1-200 keV range (Grandi et al. 1997). The usage of the ratio washes out in principle any problem regarding instrumental calibration and the - until now not deeply studied - relative calibration between ROSAT and Beppo-SAX instruments. Moreover, it allows the use of an extended energy range of both instruments, where the response matrices are currently not well calibrated yet, but where a significant amount of counts still exists. A PSPC 3C273 spectrum has been extracted from a pointing observation included in the public archive. The spectral ratios are shown in Fig. 6. MECS spectrum remains pretty flat till $\simeq$ 1 keV, being inconsistent with the PSPC one also in the extended energy range, where the PSPC flux is $\sim$ 3 times higher. Such a difference cannot be explained in terms of spectral pivoting; in such a case the pivot should lie at $E \simeq 5.4$ keV, while we found no evidence of spectral steepening in the Beppo-SAX data.

In Fig. 7 the X-ray SED of the PSPC (0.1-2.4 keV) and MECS (1,5-10.5 keV) data is plotted, together with one ASCA

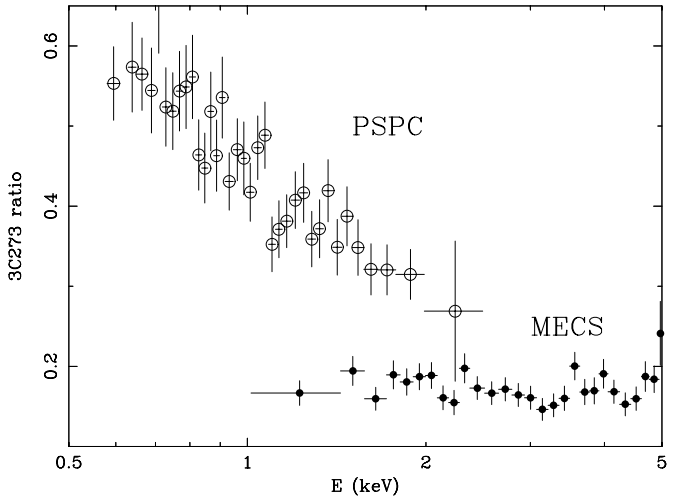

Fig. 6. Ratio of the PSPC (*open circles*) and MECS (*filled circles* spectra with the relevant 3C273 spectra. Each point corresponds to a S/N > 10

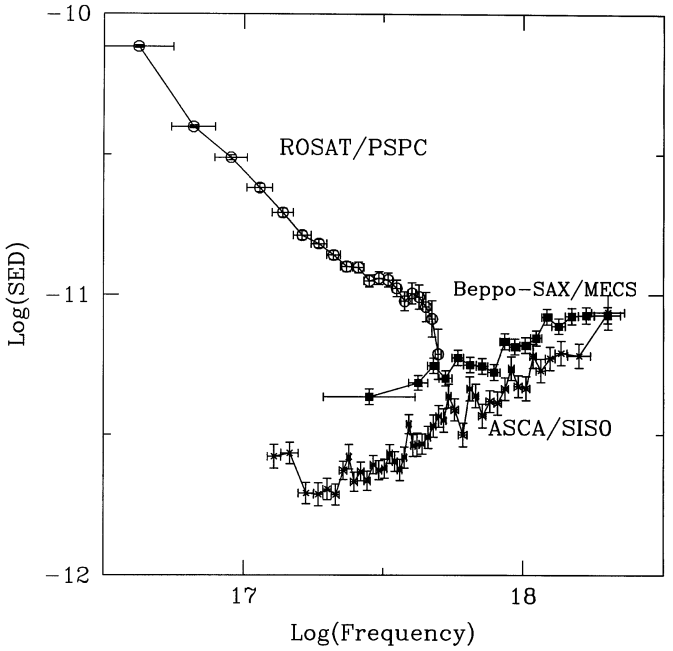

Fig. 7. X-ray SED (νF_ν in units of erg cm^{-2} s^{-1} Hz^{-1}) of the ROSAT/PSPC, Beppo-SAX/MECS and 1996 July ASCA/SIS0 observations

(0.5-10 keV) observation performed during summer 1996 (a complete analysis of the ASCA data is included in Turner et al. 1998). ASCA spectrum is consistent with and rather flat ($\Gamma = 1.4 - 1.6$) power-law in the whole 0.7-10 keV band and a soft excess at lower energies, although with a much lower flux than the PSPC spectrum (Turner et al. 1998). The 0.7-2 keV spectrum had undergone a transition from a steep ($\Gamma \gtrsim 2.5$) to a flat ($\Gamma \simeq 1.55$) state. Two possible explanations are viable to account for the observed behavior. 1H0419-577 could display a remarkably variable soft excess. Alternatively, ROSAT and Beppo-SAX could have monitored two different states of the nuclear primary continuum source.

6. Discussion

1H0419-577 displays a combination of X-ray continuum and line properties which is somewhat at odds with other Seyfert 1s. A simple power-law is a good description of the data in the whole 1.8-40 keV band, with a rather flat index ($\Gamma = 1.55$). Both thermal and non-thermal Comptonization models can produce such flat spectra (Svensson 1994, Haardt et al. 1997), although in rather extreme conditions. No iron emission line was detected: the upper limit on the EW of a narrow (broad) iron line from neutral iron is $\sim$90 (250) eV. We extrapolated from the ASCA Nandra et al. (1997a) sample the 5 objects whose 3-10 keV photon index is consistent with 1H0419-577 one within the statistical uncertainties (cfr. Table 2 in their paper: NGC3227, NGC3783, Mrk841, NGC6814 and MCG-2-58-22). The average observed EW in these objects (121 ± 16) is significantly higher then the 1H0419-577 upper limit. The constraints on the line properties are however not very tight. It is worthwhile to notice that the line upper limits are consistent, within the statistical uncertainties, both with the EW vs. luminosity anti-correlation discovered by Nandra et al. (1997b) and with the line detected in the ASCA spectrum by Turner et al. (1998).

The 1H0419-577 2-10 keV luminosity is $\sim 5 \times 10^{44}$ erg s^{-1}, which points to a borderline case between Seyferts and quasars. The lack of Compton reflection and/or fluorescent iron line in the X-ray spectra of quasars is still puzzling, given the fact that these features seem almost universal in low luminosity objects. A possible explanation assumes that the disk surrounding the central black hole becomes substantially ionized when the primary luminosity increases (Matt et al. 1993). That would decrease the contrast between reflected and direct continua and shift the line emission centroid towards energies corresponding to ionized iron stages; eventually, the intensity of the iron line would fade away when iron turns more and more into a completely ionized stage. No ionized line or Compton reflection are required by the 1H0419-577 data, but the constraints on the spectral parameters are again too loose.

The comparison between MECS results and 1992 ROSAT and 1996 ASCA observations demonstrates that *at least* the 0.5-2.5 keV has changed by a factor of ~ 6 in flux while turning from a soft ($\Gamma_{PSPC} \gtrsim 2.5$) to a hard ($\Gamma_{MECS} \simeq 1.55$) state. ASCA data suggested the presence of a soft excess above the extrapolation of a rather hard high-energy power-law below 0.7 keV (Turner et al. 1998), which would have had a much lower flux and/or effective temperature than observed by ROSAT. Some authors (Walter & Fink 1993, Puchnarewicz et al. 1996) suggested that the optical to soft X-ray continuum could be seen as part of the same "Big Bump" (BgB), to which a hard power-law with typical $\Gamma = 2$ is underlying. Variability by a factor of $\sim$few seems to be a common property of soft X-ray radio-quiet AGN (Mannheim et al. 1996) It was recently suggested that such a variability is connected to the transient nature of disk emission around 10^6-10^7 $M_\odot$ black holes with near-Eddington accretion

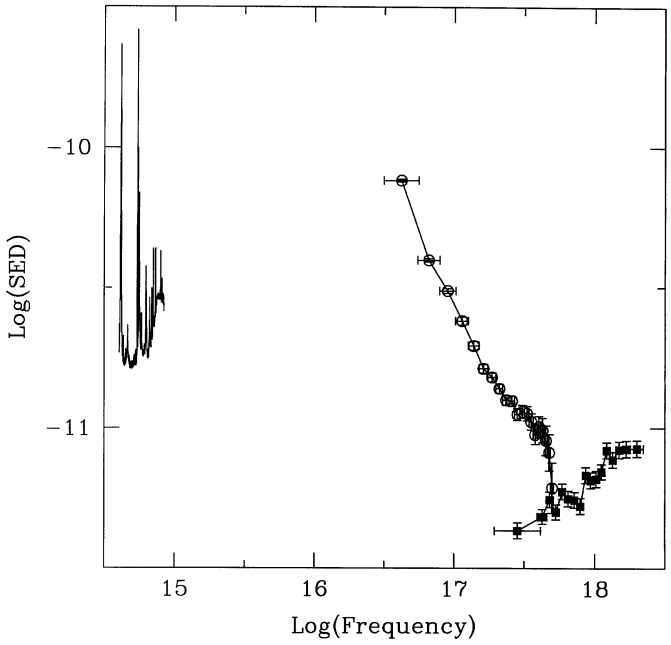

Fig. 8. Optical to X-ray SED. Both Beppo-SAX MECS (*filled circles*) and ROSAT/PSPC (*empty squares*) data are shown together with the Beppo-SAX simultaneous optical spectrum

(Grupe et al. 1998). In order to qualitatively check these scenarios, we show the optical to X-ray SED in Fig. 8. Simultaneous MECS and optical data seem to suggest that the peak of the energy density lies around $\sim 3500-4000$ Å, as typically observed in Radio Quiet Quasars (RQQ, Laor et al. 1997). If the PSPC data represents a soft excess which is still present also at the epoch of the Beppo-SAX observation, a simple extrapolation of the data suggests that such a soft excess cannot be reconnected in a single component with the optical to hard X-ray spectrum. The soft X-rays are clearly variable, and a corresponding dynamics of the optical/UV emission are required to occur as well if the optical emission is tightly related to it. However, strong variations in the optical band have not been observed yet.

A way to characterize the soft X-ray and optical properties of QSO is through the multiwavelength “point-to-point” spectral indices α_{ox} and α_{os}. We follow hereinafter the definition by Laor et al. (1997), where $\alpha_{os} = [\log(f_{0.3\ keV}/f_{3000\text{Å}})]/1.861$ and $\alpha_{ox} = [\log(f_{2\ keV}/f_{3000\text{Å}})]/2.685$ (f is the flux density). We extrapolated the density flux at 3000Åfrom the optical spectrum presented in Sect. 2. For 1H0419-577 $\alpha_{os} = -0.93$ and $\alpha_{ox} = -1.23$. These values are in good agreement with the outcomes of the RIXOS sample analysis (Puchnarewicz et al. 1996), but flatter than in the complete PG sample of Wilkes et al. (1994) and in the optically selected sample of Laor et al. (1997) (for both $\alpha_{ox} \simeq -1.5$). A possible explanation for this discrepancy is that optically selected samples tend to be biased in favor of objects with intense optical/X-ray ratios. 1H0419-577 α_{ox} is also consistent, within the statistical dispersion, with Walter & Fink sample (1993, $\alpha_{ox} = -1.37 \pm 0.23$), which is selected upon the X-ray brightness (the difference in α_{ox} induced by the different choice of the reference optical energy between Laor et al. (1997) and Walter & Fink (1993) - 3000Åvs. 2650Å- is well within the statistical dispersion).

The four year variation timescale implies that the soft excess emission region is smaller than 1 pc, and therefore associated with the nuclear region, where the primary continuum is expected to undergo strong reprocessing. If reprocessing is the ultimate cause of the soft excess, the energy balance requires that any cut-off is confined at energies $\gtrsim 100$ keV; that does not contrast the average behavior of Seyfert galaxies (Gondek et al. 1996). Any change of the flux/temperature of the soft excess has to be causally related to the variation of the high-energy spectrum. The lack of response of the soft X-rays to a $\Gamma \sim 0.2$ change of the 0.7-10 keV photon index within two weeks (Turner et al. 1998) puts any reprocesser farther than 10^4 Schwarzschild radii from a $10^7\ M_\odot$ black hole. Domination of scattering in the soft X-ray emission is unlikely because of the variability in the PSPC and HRI data (Turner et al. 1998).

An appealing alternative possibility is that the difference between the measured steepness of the PSPC and MECS spectra ($\Delta\Gamma > 0.9$) is due to a change of the primary continuum itself. Haardt & Maraschi (1993) have shown that a disk corona, Comptonizing the soft photons supplied by a Shakura-Sunayev disk, can naturally reproduce the medium X-ray spectra shape typically observed in Seyfert 1. Interestingly enough, Γ_{hard} and Γ_{soft} in 1H0419-577 are very close to the expected spectral indices if the coronal plasma undergoes a transition between a scattering optically thin ($\tau \lesssim 1$, $\Gamma = 1.55$) and thick ($\tau \sim 1$, $\Gamma = 2.5$) regime (Haardt, Maraschi & Ghisellini, 1997). A pair dominated corona would require an increase of the 2-10 keV flux by more than 4 orders of magnitude for a steepening $\Delta\Gamma \sim 1$ to be achieved. On the contrary, if we extrapolate the PSPC best fit power-law into the 2-10 keV band, the luminosity is $\sim 4.8 \times 10^{44}$ erg s^{-1}, which is comparable with the MECS measurement. A pair-saturated plasma can be therefore ruled out. A measurable side-effect in such a scenario would be an increase by an order of magnitude of the ratio between the flux in the 2-10 keV band above $E \gtrsim 30$ keV. The hypothesis of a change of the Comptonized spectral shape could provide also a good explanation for the relative faintness of the iron line emission, if the Compton component responds not simultaneously to the - basically unknown - pattern of variability of the primary emission.

Another possibility to explain a change in the primary continuum spectral shape comes from the analogy between Seyfert galaxies and Black Hole Candidates (BHC). BHC are well know to display two different intensity and spectral states: a high and soft one, characterized above ~ 10 keV by a power-law spectrum with photon index $\simeq 2.5$, and a low and hard one, with typical $\Gamma \sim 1.3-1.9$. Such an analogy had been first suggested to explain the very soft ($\Gamma \simeq 2.6$) ASCA spectrum of the NLSy1 galaxy RE1034+39 (Pounds et al. 1995).

Ebisawa et al. (1996) have recently suggested that the difference between the two states is due to different Comptonization mechanisms in a viscuosless shock two-phase accretion disc. Thermal Comptonization in a disk with a very low accretion

rate (and therefore low thermal soft emission) would yield a hard spectrum with $\Gamma \sim 1.5$, regardless of the *absolute* black hole mass. If, however, the accretion rate increases, more soft photons are supplied, and the post-shock region cooling becomes more efficient. The cooler inflow towards the nuclear black hole is responsible for a steep non-thermal emission. The resulting spectrum in a quasi-Eddington regime is the combination of the thermal emission from the optically thick disk and of a power-law with $\Gamma \sim 2.5$. In this framework, the observed variability pattern in 1H0419-577 would therefore suggest a transition phase from a bulk motion to a thermal motion regime due to a change of the accretion rate. Typical kT_{BB} in BHC in high state are ~ 1 keV; scaling $T_B \propto M^{1/4}$, a blackbody temperature $\lesssim 80\,eV$ corresponds to a black body mass $M_{BH} \gtrsim 2 \times 10^6\ M_\odot$. The bolometric luminosity of the blackbody component as measured by PSPC on 1H0419-577 is $\sim\ 5 \times 10^{44}\ erg\ s^{-1}$ and self-consistently in this case $\dot{m}/\dot{m}_{Edd} \sim 1$. However, it must be kept in mind that the determination of a blackbody temperature sensitively depends on the energy band where the spectral fits are performed and that the spectral deconvolution in the PSPC spectra of 1H0419-577 is not unique. We are then far from considering this coincidence as a confirmation of the proposed scenario.

7. Summary

We report on the first simultaneous X-ray and optical observations of the radio-quiet AGN 1H0419-577. The main results can be summarized as follows:
(1) the optical spectrum points unambiguously to a classification as a Seyfert 1.
(2) 1H0419-577 is detected in X-rays up to 40 keV. The whole 1.8-40 keV spectrum is well modeled by a simple power-law with a rather flat ($\Gamma \simeq 1.55$) spectral index.
(3) No iron emission line or Compton reflection by an X-ray illuminated neutral disc are required by the data. However, the constraints on the spectral parameters are not so tight to rule out the possibility that this object follows the trend of high luminosity Seyferts to have fainter and/or ionized iron lines and Compton continua.
(4) The SED of the simultaneous optical and X-rays observations peaks apparently around 3500-4000Å, as typically observed in RQQ (Laor et al. 1997).
(5) The comparison with a 1992 ROSAT and a pair of 1996 ASCA observations (Turner et al. 1998) reveals that the spectrum has undergone a transition between a soft ($\Gamma \gtrsim 2.5$) and a hard ($\Gamma \simeq 1.55$) state, *at least* in the 0.7-2 keV band. We have discussed in this paper two possible explanations for this behavior and their implications:

- a remarkably variable ($\sim$ half an order of magnitude in flux and/or effective temperature) soft X-ray excess, which should come along with a corresponding dynamics of the optical and UV emission, if the SED is dominated by a single BgB. The optical historical monitoring of this source, albeit sparse, seems to rule out this possibility;
- a change of the primary continuum spectrum, which could be explained either as a transition from a Compton thick to a Compton thin regime in the disk-corona two-phase model of Haardt & Maraschi (1993) or a transition between a bulk to a thermal motion regime in a viscuosless two-phase shock accretion disc (Chakrabarti and Titarchuk 1995; Ebisawa et al. 1996).

Acknowledgements. The authors would like to warmly thank the whole Beppo-SAX team, whose intelligent and hard work made possible this observation to be successfully performed. The authors acknowledge valuable suggestions from M.Cappi, P.Giommi and F.Haardt and a careful revision of the manuscript by S.Kaiser. M.G. acknowledges an ESA Research Fellowship. A.C. and G.M.S. acknowledge financial support from ASI contract ARS96-70. This work has made use of the NASA/IPAC Extragalactic Database (NED), which is operated by the Jet Propulsion Laboratory, Caltech, under contract with N.A.S.A., and of the cleaned and linearized event files produced at the Beppo-SAX Science Data Center.

References

Arnaud K.A., Branduardi-Raymond G., Culhane J.L., et al., 1985, MNRAS 217 105
Boella G., Perola G.C., Scarsi L., 1997a, A&AS 122, 299
Boella G., Chiappetti L., Conti G., et al., 1997b, A&AS 1997, 122, 327
Brissenden R.J.V., 1989, PhD thesis, Australian National University
Chakrabarti S., Titarchuk L., 1995, ApJ 455, 623
Clavel J., Reichert G.A., Alloin D., et al., 1991, ApJ 366, 64
Cusumano G., Mineo T., Segreto A., et al., 1998, Proceedings of the Symposium "The active sky: first results from Beppo-SAX and RXTE", Scarsi L., Bradt H., Giommi P., Fiore F. eds., in press
Czerny B., Elvis M., 1987, ApJ 321, 305
Dickey J.M., Lockman F.J., 1990, ARA&A 28, 215
Ebisawa K., Titarchuk L., Chakrabarti S.K., 1996, PASJ 48, 59
Fiore F., Elvis M., McDowell J.C., et al., 1994, ApJ 431, 515
Frontera F., Costa E., Dal Fiume F., et al., 1997, A&AS 122, 357
Fruscione A., 1996, ApJ 459, 509
Grandi P., Guainazzi M., Mineo T., et al., 1997, A&A 325, 17
Grupe D., 1996, Ph.D thesis, University of Göttingen
Grupe D., Beuermann K., Thomas H.-C., Mannheim K., Fink H.H., 1998, A&A in press (available at astroph/9710298)
Gondek D., Zdziarski A.A., Johnson W.N., et al. 1996, MNRAS 282, 646
Guainazzi M., Comastri A., Stirpe G., et al., 1998, Proceedings of the Symposium "The active sky: first results from Beppo-SAX and RXTE", Scarsi L., Bradt H., Giommi P., Fiore F. eds., in press (available at astro-ph/9712248)
Guainazzi M., Matteuzzi A., 1997, SDC TR-011 (available at `ftp://www.sdc.asi.it/pub/docs/sdc_tr011.ps`)
Haardt F., Maraschi L., 1993, ApJ 413, 507
Haardt F., Maraschi L., Ghisellini G., 1997, ApJ 476, 620
Joly M., 1988, A&A 192, 87
Kruper J., Urry C.M., Canizares C.R., 1990, ApJS 74, 347
Iwasawa K., Fabian A.C., Brandt W.N., 1998, MNRAS in press (available at astroph/9708133)
Laor A., Fiore F., Elvis M., et al., 1997, ApJ 477, 93
Mannheim K., Grupe D., Beuermann K., et al., 1996, Proceedings "Röntgenstrahlung from the Universe", H.U.Zimmermann, J.Trümper and H.Yorke eds., MPE Report 263, p. 471
Manzo G., Giarrusso S., Santangelo A., et al., 1997, A&AS 122, 341

Marshall H.L., Fruscione A., Carone T.E., 1995, ApJ 439, 90
Matt G., Fabian A.C., Ross R.R., 1993, MNRAS 262, 179
Molendi S., Maraschi L., Stella L., 1992, MNRAS 255, 27
Mushotzky R.F., 1984, Adv. Space Res. 3, 157
Nandra K., George I.M., Mushotzky R.F. et al., 1997a, ApJ 477, 602
Nandra K., George I.M., Mushotzky R.F. et al., 1997b, ApJL 488, L91
Nandra K., Pounds K.A., 1994, MNRAS 268. 405
Parmar A., Martin D.D.E., Bavdaz M., et al., 1997, A&A 122, 309
Peterson B.M., Bolonek T.S., Barker E.S., et al., 1991, ApJ 368, 119
Piro L., Balucinska-Church M., Fink F., et al., 1997, A&A 319, 74
Piro L., Yamauchi M., Matusoka M., et al., 1990, ApJL 360, L35
Pounds K., Done C., Osborne J.P., 1995, MNRAS 277, L5
Pounds K., Nandra K., Stewart G.C., et al., 1990, Nat 344, 132
Pravdo S.H., Nugent J.J., Nousek J.A., et al., 1981, ApJ 251, 501
Puchnarewicz E.M., Mason K.O., Romero-Colmenero E., et al., 1996, MNRAS 281, 1243
Siemiginowska A., Kuhn O., Elvis M., et al., 1995, ApJ 454, 77
Singh K., Garmire G.P., Nousek J., 1985, ApJ 297, 633
Svensson R., 1994, ApJS 92, 585
Tanaka Y, Nandra K., Fabian A.C., et al., 1995, Nat 375, 659
Turner T.J., 1993, in “The 1st annual ROSAT Science Symposium and Data Analysis”, University of Maryland
Turner T.J., George I.M., Grupe D., et al., 1998, ApJ in press (available at astroph/9807142)
Turner T.J., Weaver K.A., Mushotzky R.F., 1993, ApJ 412, 72
Turner T.J., Williams O.R., Courvoisier T. J.-L., et al., 1990, MNRAS 244, 310
Turner T.J., Pounds K.A., 1989, MNRAS 240, 833
Ulrich M.-H., Molendi S., 1995, A&A 293, 641
Walter R., Fink H.H., 1993, A&A 275, 105
Wilkes B., Tananbaum H., Worral D., et al., 1994, ApJS 92, 53